ChemComm

COMMUNICATION

View Article Online
View Journal | View Issue



Cite this: *Chem. Commun.*, 2021, **57**, 7374

Received 31st May 2021,
Accepted 29th June 2021

DOI: 10.1039/d1cc02873a

rsc.li/chemcomm



# Synergistic covalent-and-supramolecular polymers connected by [2]pseudorotaxane moieties†

Junjun Wan, ‡ Zhaoming Zhang,*‡ Yongming Wang, Jun Zhao, Yumeng Qi, Xinhai Zhang, Kai Liu, Chunyang Yu* and Xuzhou Yan*

**Synergistic covalent-and-supramolecular polymers, in which covalent polymers and supramolecular polymers connect with each other through [2]pseudorotaxane moieties, are designed and synthesized. The unique topological structure effectively enhances the synergistic effect between these two polymers, thereby generating a novel class of mechanically adaptive materials.**

Polymers have garnered a ubiquitous presence in our daily life. Most polymer materials could be classified into covalent polymers (CPs) which exhibit stable properties and remarkable strength but a lack of dynamic behavior. On the contrary, supramolecular polymers (SPs) whose monomers are connected by non-covalent interactions have a notable performance in terms of stimuli-responsiveness and self-adaptivity *etc.*, whereas they also suffer from poor mechanical properties.[1] Due to these inherent features, it is still limited for polymers to prepare specific materials, for example, materials with good mechanical adaptivity and robustness. Recently, we have developed synergistic covalent-and-supramolecular polymers (CSPs), in which CPs and SPs interact with each other to form relatively fixed structures and behave as a whole to determine the properties and implement the functions. Benefiting from the effective integration of the two kinds of polymers, the materials based on CSPs exhibit robust yet dynamic properties, thereby filling the gap between CPs and SPs.[2] To date, there are only a few examples on the construction of synergistic CSPs.[2,3] Therefore, it is highly desirable to develop novel synergistic CSPs with creative architectures and emergent features and functions, which would be favorable to enrich the CSP system.

The synergy between CPs and SPs largely determines the mechanical performance of CSPs. From the structural point of view, the synergistic effect in CSPs is related to the interactions between CPs and SPs. In our previous work, covalent bonding and noncovalent quadruple H-bonding have been utilized to connect CPs and SPs. Covalent bonding could guarantee an efficient synergistic effect because of its high strength and thus endow the CSPs with remarkable mechanical properties.[2a] Quadruple H-bonding junctions make the resultant CSPs more dynamic and tough due to the outstanding energy dissipative abilities.[2b] These results indicated that the connection types between CPs and SPs play a crucial role in modulating the mechanical properties of CSPs. As such, it is worth developing CSPs with new junctions.

[2]Pseudorotaxanes, one of the most popular structures in supramolecular chemistry, contain a wheel-like host and a guest axle.[4] They represent not only a kind of supramolecular interaction but also a special topological structure.[5] We speculate that the use of [2]pseudorotaxane as a junction would bring new features to CSPs. Herein, we report a *de novo* chemical design of synergistic CSPs in which CPs and SPs are connected by crown ether-based [2]pseudorotaxane moieties. Due to the unique combination of CPs, SPs, and [2]pseudorotaxane junctions, the representative CSP not only gelates at a suitable concentration ($>29.6$ mg mL$^{-1}$) at room temperature but also exhibits good mechanical properties in terms of Young's modulus (116 MPa), maximum stress (12 MPa), and stretchability ($\sim$400%) in the bulk.

As shown in Fig. 1, the covalent polymer (CP-**1**) adopted here is a crown ether-functionalized polynorbornene derivative prepared by ring-opening metathesis polymerization (ROMP), which has high stability and shows good performance in the construction of elastomers.[2] CP-**1** was first mixed with a bis(pyridinium) ligand in $CH_3CN/CHCl_3$ (3 : 1, v/v) solution. Driven by the host–guest recognition, the ligand threaded into the benzo-24-crown-8 (B24C8) wheel on CP-**1** to form a side-chain poly[2]pseudorotaxane (CP-**2**).[6] Subsequently, bis(benzonitrile)palladium dichloride ($Pd(PhCN)_2Cl_2$) was introduced to coordinate with the bis(pyridinium) ligand to afford SP,[7] which connected with CP-**1** by [2]pseudorotaxane moieties to form a new class of synergistic

*School of Chemistry and Chemical Engineering,*
*Frontiers Science Center for Transformative Molecules,*
*Shanghai Jiao Tong University, Shanghai 200240, P. R. China.*
*E-mail: zhangzhaoming@sjtu.edu.cn, chunyangyu@sjtu.edu.cn, xzyan@sjtu.edu.cn*

† Electronic supplementary information (ESI) available. See DOI: 10.1039/d1cc02873a

‡ These authors contributed equally to this work.

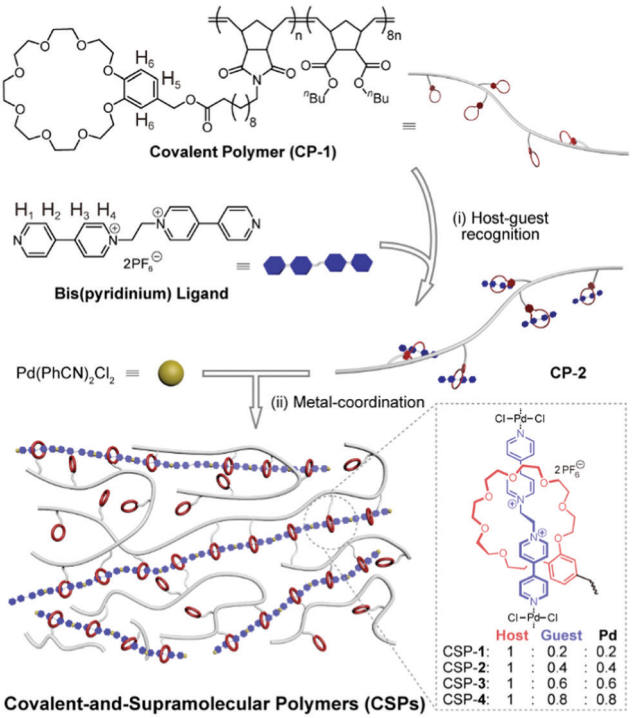


Fig. 1 Schematic representation of the formation of synergistic CSPs and chemical structures of the CP-**1** and bis(pyridinium) ligand.

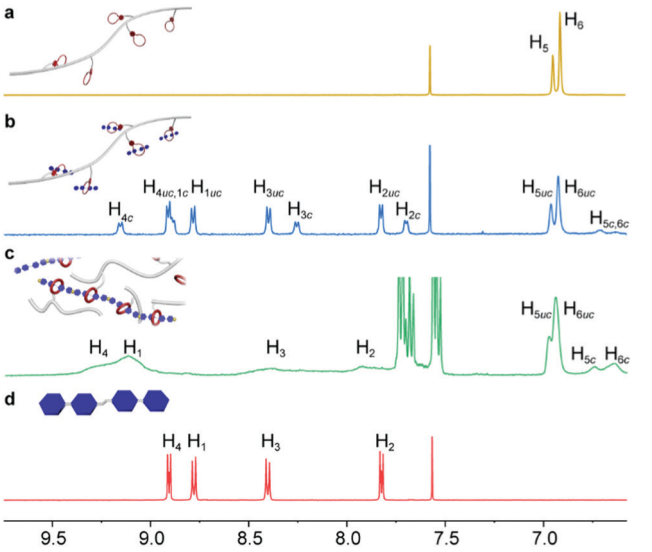


Fig. 2 Partial $^1$H NMR (400 MHz, $CD_3CN:CDCl_3$ = 3 : 1 v/v, 298 K) of (a) CP-**1**, (b) CP-**2**, (c) CSP-**2** and (d) the bis(pyridinium) ligand. Letters "c" and "uc" denote complexed and uncomplexed species, respectively.

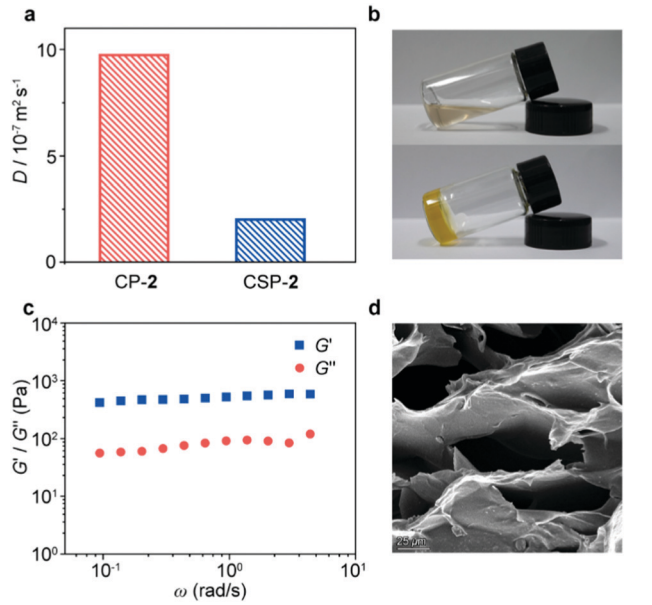


Fig. 3 (a) Diffusion coefficient $D$ (500 MHz, $CD_3CN/CDCl_3$ = 3 : 1 v/v, 298 K) of CP-**2** and CSP-**2**. (b) Images of CP-**2** solution (above) and CSP-**2** gel (below). Solvent: $CH_3CN:CHCl_3$ = 3 : 1 v/v, 2.0 mL. (c) Storage modulus $G'$ and loss modulus $G''$ *versus* frequency ($\omega$) for the CSP-**2** gel. (d) The SEM image of the freeze-dried CSP-**2**.

CSPs. It is worthy of note that the feed ratios of the bis(pyridinium) ligand and $Pd(PhCN)_2Cl_2$ were always equal, but their ratio to the B24C8 moiety was set as 0.2, 0.4, 0.6, and 0.8, which corresponded to CSPs-**1**–**4**, respectively (Fig. 1).

The formation of CSPs was first investigated by using $^1$H NMR spectra. After mixing with CP-**1**, the characteristic signals of the bis(pyridinium) ligand had noticeable chemical shifts (Fig. 2b and d), which kept the same when mixed with the B24C8 monomer (Fig. S15, ESI†), suggesting the formation of [2]pseudorotaxane units on the side chain of CP-**1**. Notably, both complexed and uncomplexed peaks were present in the spectrum, which could be ascribed to the slow exchange nature of the host–guest recognition.[8] Upon the addition of $Pd(PhCN)_2Cl_2$ into the mixture, the proton signals of the bis(pyridinium) ligand became much broader (Fig. 2c), indicative of supramolecular polymerization driven by metal coordination. The assignment of the corresponding peaks was assisted by using the 2D COSY NMR spectrum of the model molecules (Fig. S16, ESI†). Moreover, the transition from linear CP-**2** to cross-linked CSP-**2** induced by Pd(II) coordination was also confirmed by using 2D DOSY NMR spectroscopy. After the addition of $Pd(PhCN)_2Cl_2$, the weight–average diffusion coefficient of the samples decreased from $9.70 \times 10^{-7}$ to $1.97 \times 10^{-7}$ $m^2$ $s^{-1}$ (Fig. 3a), which implied the formation of a cross-linked structure.

When $Pd(PhCN)_2Cl_2$ was added to the CP-**2** solution to form CSP-**2**, the gelation phenomenon was observed (>29.6 mg $mL^{-1}$, Fig. 3b). The rheology measurement showed that the storage modulus ($G'$) of the gel was higher than the loss modulus ($G''$) in the measured frequency range (Fig. 3c), which exhibited a good elastic behavior and implied the existence of an effective network structure.[9] The SEM image of the corresponding freeze-dried gel exhibited an interconnected porous morphology (Fig. 3d), reflecting the microstructure of the CSP gel. In addition, the STEM image of CSP-**2** revealed discrete distributions of palladium element (Fig. S17, ESI†). It means that there is an effective interaction between SPs and CPs to restrict the aggregation of SPs.

Thermogravimetric analysis (TGA) showed that all the samples had good thermal stability with decomposition temperatures

above 200 °C (Fig. S18, ESI†). Differential scanning calorimetry (DSC) was also employed for the sample analysis (Fig. 4a). The glass transition temperature ($T_g$) values of CP-**1** and CSPs-**1–4** were measured to be −16.1, −14.7, −7.3, −3.9, and 7.5 °C, respectively. There was a tendency that $T_g$ increased with the increase of SP content because of the enhanced crosslinking density of the network. Besides, transitions located around 46 °C were also found on the DSC curves of CSPs-**2–4**, which might be related to metal-coordination-driven supramolecular polymerization.

Subsequently, the tensile tests of CSPs-**1–4** were performed, and the corresponding results are displayed in Fig. 4b. All CSPs exhibited obvious and regular yielding behaviors. With the increase of SP content, the strength of the CSPs increased gradually, but their elongation became lower (Table S1, ESI†). Due to the moderate mechanical performance (Young's modulus = 116 MPa, maximum stress = 12 MPa, and stretchability = 400%), CSP-**2** was selected for further study. Its comparison with the mechanical properties of CP-**2** is shown in Fig. 4c. As a side-chain poly[2]pseudorotaxane, CP-**2** was highly stretchable (>1000%), but possessed a poor stiffness (Young's modulus = 0.48 MPa) and strength (maximum stress = 0.12 MPa). It is obvious that the overall mechanical properties of CSP-**2** were much superior to those of CP-**2**, which indicated the important role of SPs in enhancing mechanical properties.

To date, the above results have revealed that SPs play an important role in the mechanical performance of CSPs. As proposed in our previous work, the dissociation of SPs upon stress could dissipate energy to modulate the mechanical behaviors of CSPs. However, the realization of this function highly depends on the interactions between CPs and SPs because force transmission needs an effective network structure. Therefore, the study on the mechanical behavior of the SP component in CSPs is also beneficial to reveal the role of the [2]pseudorotaxane junction. To this end, tensile tests with different deformation rates were carried out (Fig. 5a). The mechanical properties of CSP-**2** exhibited a high dependence on stretching rate, especially Young's modulus varied from ~70 to ~150 MPa (Table S2, ESI†), consistent with the involvement of dynamic SPs.

The relaxation tests of CSP-**2** with different fixed strains displayed an unusual trend (Fig. 5b), which was exhibited by summarizing the residual stresses shown in Fig. 5c. Moreover, the CSP-**2** samples upon stress relaxation tests were further applied to tensile tests to investigate their structure changes (Fig. 5d). At the small strains of 3% and 5%, their residual stresses in the relaxation tests were almost the same, and the mechanical behaviors of the two samples were similar to the original CSP-**2** sample. These results implied that the network under these strains was intact. When the strain increased from 5% to 20%, the curve of the residual stresses decreased with a fixed slope, which probably indicated the dissociation of SPs. However, the mechanical properties of the samples such as Young's modulus have no significant changes, and only the elongation at break went down slightly (Fig. S20, ESI†). It could be speculated that the damage of SPs started to occur in this stage but only small amounts of the coordinate bond were broken. Notably, the dissociation of SPs at a small strain of 7% suggested that the [2]pseudorotaxane junction could combine CPs and SPs tightly to form a network and achieve an efficient

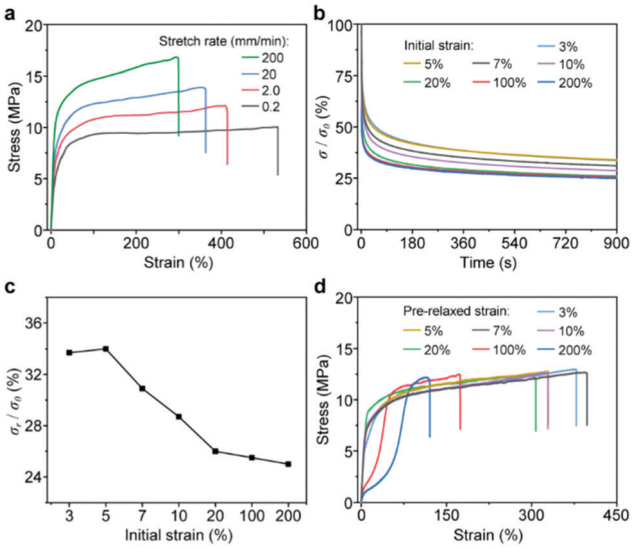


Fig. 5 (a) Tensile stress–strain curves of CSP-**2** with different deformation rates. (b) Normalized stress relaxation curves of CSP-**2** with different initial strains. (c) The normalized residual stress $\sigma_r$ of CSP-**2** with different initial strains. (d) Tensile stress–strain curves of CSP-**2** samples after being pre-relaxed with different strains.

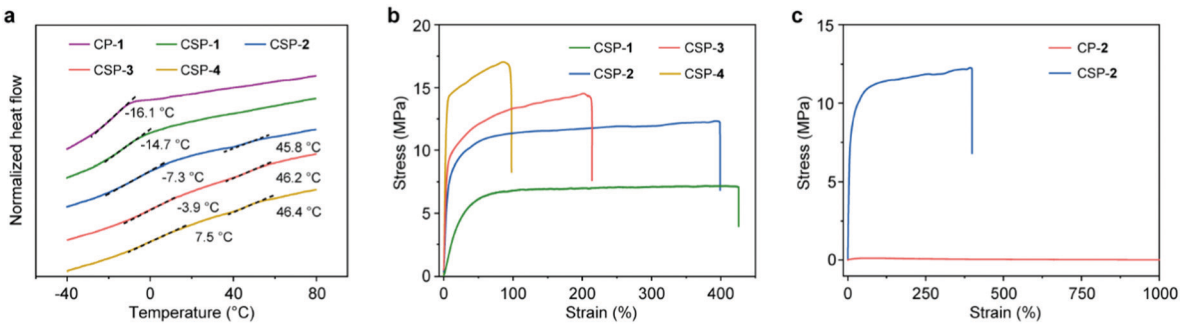


Fig. 4 (a) DSC curves of CP-**1** and CSPs-**1–4** recorded by heating scan from −40 to 80 °C with a heating rate of 20 °C min$^{-1}$. (b) Tensile stress–strain curves of CSPs-**1–4** in the bulk. Deformation rate: 20 mm min$^{-1}$. (c) Tensile stress–strain curves of CP-**2** and CSP-**2** samples in the bulk. Deformation rate: 20 mm min$^{-1}$.

 

synergistic effect. After the initial strain increased up to 100% and 200%, the slope of the residual stress curve became slower (Fig. 5c), and the mechanical properties including Young's modulus, yield strength, and fracture strain decreased significantly. Under these loaded strains, the extensive dissociation of SPs might take place. But even though the SPs broke into a large number of fragments, the materials with the remaining network structure still maintained high breaking strength, which indicated that the [2]pseudorotaxane junction is able to make full use of the SPs to modulate the mechanical properties. A cyclic tensile test and strain sweep rheological test were also performed to confirm our speculation (Fig. S21 and S22, ESI†).

In summary, we have designed and prepared a series of synergistic CSPs with [2]pseudorotaxane junctions by successive covalent and supramolecular polymerizations. The gelation phenomenon and characterization on the gel confirmed that the CSPs have obvious network structures. In tensile tests, the representative CSP-**2** exhibited good mechanical properties in terms of stiffness (Young's modulus = 116 MPa), strength (maximum stress = 12 MPa), and stretchability (~400%). The combined experiments of stress relaxation and subsequent tensile tests disclosed that the SPs started to dissociate at a relatively small strain (~7%) and still contributed to the mechanical performance after being fractured by large strains (~200%). The achievement of these behaviors for SP benefits from the effective connection enabled by [2]pseudorotaxane moieties. This work develops a new CSP structure, and we anticipate that it could be beneficial to facilitate the advancement and application of synergistic CSP materials.

X. Y. acknowledges financial support from the NSFC/China (21901161 and 22071152) and the Natural Science Foundation of Shanghai (20ZR1429200).

## Conflicts of interest

There are no conflicts to declare.

## Notes and references

1 (*a*) T. F. A. De Greef, M. M. J. Smulders, M. Wolffs, A. P. H. J. Schenning, R. P. Sijbesma and E. W. Meijer, *Chem. Rev.*, 2009, **109**, 5687–5754; (*b*) G. Yu, K. Jie and F. Huang, *Chem. Rev.*, 2015, **115**, 7240–7303; (*c*) M. J. Webber, E. A. Appel, E. W. Meijer and R. Langer, *Nat. Mater.*, 2016, **15**, 13–26; (*d*) D. W. Balkenende, C. A. Monnier, G. L. Fiore and C. Weder, *Nat. Commun.*, 2016, **7**, 10995; (*e*) X. Wang, Y. Han, Y. Liu, G. Zou, Z. Gao and F. Wang, *Angew. Chem., Int. Ed.*, 2017, **56**, 12466–12470; (*f*) H. Chen, Z. Huang, H. Wu, J. F. Xu and X. Zhang, *Angew. Chem., Int. Ed.*, 2017, **56**, 16575–16578; (*g*) S. Wang, Z. Xu, T. Wang, T. Xiao, X. Y. Hu, Y. Z. Shen and L. Wang, *Nat. Commun.*, 2018, **9**, 1737; (*h*) Q. Zhang, Y. X. Deng, H. X. Luo, C. Y. Shi, G. M. Geise, B. L. Feringa, H. Tian and D. H. Qu, *J. Am. Chem. Soc.*, 2019, **141**, 12804–12814; (*i*) K. Liu, Y. Jiang, Z. Bao and X. Yan, *CCS Chem.*, 2019, **1**, 431–447; (*j*) L. Wang, L. Cheng, G. Li, K. Liu, Z. Zhang, P. Li, S. Dong, W. Yu, F. Huang and X. Yan, *J. Am. Chem. Soc.*, 2020, **142**, 2051–2058; (*k*) D. Xia, P. Wang, X. Ji, N. M. Khashab, J. L. Sessler and F. Huang, *Chem. Rev.*, 2020, **120**, 6070–6123; (*l*) G. Li, L. Wang, L. Wu, Z. Guo, J. Zhao, Y. Liu, R. Bai and X. Yan, *J. Am. Chem. Soc.*, 2020, **142**, 14343–14349; (*m*) B. Tang, W. Xu, J.-F. Xu and X. Zhang, *Angew. Chem., Int. Ed.*, 2021, **60**, 9384–9388; (*n*) H. Wang, K. Wang, Y. Xu, W. Wang, S. Chen, M. Hart, L. Wojtas, L.-P. Zhou, L. Gan, X. Yan, Y. Li, J. Lee, X.-S. Ke, X.-Q. Wang, C.-W. Zhang, S. Zhou, T. Zhai, H.-B. Yang, M. Wang, J. He, Q.-F. Sun, B. Xu, Y. Jiao, P. J. Stang, J. L. Sessler and X. Li, *J. Am. Chem. Soc.*, 2021, **143**, 5826–5835; (*o*) F. Xu, L. Pfeifer, S. Crespi, F. K.-C. Leung, M. C. A. Stuart, S. J. Wezenberg and B. L. Feringa, *J. Am. Chem. Soc.*, 2021, **143**, 5990–5997; (*p*) K. Liu, L. Cheng, N. Zhang, H. Pan, X. Fan, G. Li, Z. Zhang, D. Zhao, J. Zhao, X. Yang, Y. Wang, R. Bai, Y. Liu, Z. Liu, S. Wang, X. Gong, Z. Bao, G. Gu, W. Yu and X. Yan, *J. Am. Chem. Soc.*, 2021, **143**, 1162–1170.

2 (*a*) Z. Zhang, L. Cheng, J. Zhao, L. Wang, K. Liu, W. Yu and X. Yan, *Angew. Chem., Int. Ed.*, 2020, **59**, 12139–12146; (*b*) Z. Zhang, L. Cheng, J. Zhao, H. Zhang, X. Zhao, Y. Liu, R. Bai, H. Pan, W. Yu and X. Yan, *J. Am. Chem. Soc.*, 2021, **143**, 902–911; (*c*) Z. Shentu, Z. Zhang, J. Zhao, C. Chen, Q. Wu, L. Wang and X. Yan, *J. Mater. Chem. A*, 2021, DOI: 10.1039/D1TA02288A.

3 (*a*) Z. Yu, F. Tantakitti, T. Yu, L. C. Palmer, G. C. Schatz and S. I. Stupp, *Science*, 2016, **351**, 497–502; (*b*) X. Hou, C. Ke, Y. Zhou, Z. Xie, A. Alngadh, D. T. Keane, M. S. Nassar, Y. Y. Botros, C. A. Mirkin and J. F. Stoddart, *Chem. – Eur. J.*, 2016, **22**, 12301–12306; (*c*) M. F.-C. Romera, X. Lou, J. Schill, G. Huurne, P.-P. K. H. Fransen, I. K. Voets, C. Storm and R. P. Sijbesma, *J. Am. Chem. Soc.*, 2018, **140**, 17547–17555.

4 (*a*) M. Xue, Y. Yang, X. Chi, X. Yan and F. Huang, *Chem. Rev.*, 2015, **115**, 7398–7501; (*b*) T. L. Price and H. W. Gibson, *J. Am. Chem. Soc.*, 2018, **140**, 4455–4465; (*c*) Y. Liu, Q. Zhang, W.-H. Jin, T.-Y. Xu, D.-H. Qu and H. Tian, *Chem. Commun.*, 2018, **54**, 10642–10645; (*d*) J. Chen, Y. Wang, C. Wang, R. Long, T. Chen and Y. Yao, *Chem. Commun.*, 2019, **55**, 6817–6826; (*e*) X.-Q. Wang, W.-J. Li, W. Wang, J. Wen, Y. Zhang, H. Tan and H.-B. Yang, *J. Am. Chem. Soc.*, 2019, **141**, 13923–13930; (*f*) Z.-J. Yan, D. Wang, Z. Ye, T. Fan, G. Wu, L. Deng, L. Yang, B. Li, J. Liu, T. Ma, C. Dong, Z.-T. Li, L. Xiao, Y. Wang, W. Wang and J.-L. Hou, *J. Am. Chem. Soc.*, 2020, **142**, 15638–15643; (*g*) H. Yao, Y. M. Wang, M. Quan, M. U. Farooq, L. P. Yang and W. Jiang, *Angew. Chem., Int. Ed.*, 2020, **59**, 19945–19950; (*h*) H. Xu, M. D. Lin, J. Yuan, B. Zhou, Y. Mu, Y. Huo and K. Zhu, *Chem. Commun.*, 2021, **57**, 3239–3242; (*i*) J. Chen, Q. Meng, Y. Zhang, M. Dong, L. Zhao, Y. Zhang, L. Chen, Y. Chai, Z. Meng, C. Wang, X. Jia and C. Li, *Angew. Chem., Int. Ed.*, 2021, **60**, 11288–11293; (*j*) Y. Lei, Q. Chen, P. Liu, L. Wang, H. Wang, B. Li, X. Lu, Z. Chen, Y. Pan, F. Huang and H. Li, *Angew. Chem., Int. Ed.*, 2021, **60**, 4705–4711; (*k*) W. Liu and J. F. Stoddart, *Chem*, 2021, **7**, 919–947; (*l*) X.-K. Ma, W. Zhang, Z. Liu, H. Zhang, B. Zhang and Y. Liu, *Adv. Mater.*, 2021, **33**, 2007476.

5 (*a*) G. Hattori, T. Hori, Y. Miyake and Y. Nishibayashi, *J. Am. Chem. Soc.*, 2007, **129**, 12930–12931; (*b*) G. Yu, Z. Yang, X. Fu, B. C. Yung, J. Yang, Z. Mao, L. Shao, B. Hua, Y. Liu, F. Zhang, Q. Fan, S. Wang, O. Jacobson, A. Jin, C. Gao, X. Tang, F. Huang and X. Chen, *Nat. Commun.*, 2018, **9**, 766; (*c*) S.-J. Rao, K. Nakazono, X. Liang, K. Nakajima and T. Takata, *Chem. Commun.*, 2019, **55**, 5231–5234.

6 CP-2 is the precursor of CSP-2 and the corresponding ratio of bis(pyridinium) ligand to the B24C8 moiety of CP-1 is 0.4.

7 (*a*) C. J. Sumby, *Coord. Chem. Rev.*, 2011, **255**, 1937–1967; (*b*) J. M. Van Raden, S. Louie, L. N. Zakharov and R. Jasti, *J. Am. Chem. Soc.*, 2017, **139**, 2936–2939; (*c*) Q. Zhang, D. Tang, J. Zhang, R. Ni, L. Xu, T. He, X. Lin, X. Li, H. Qiu, S. Yin and P. J. Stang, *J. Am. Chem. Soc.*, 2019, **141**, 17909–17917; (*d*) Y. Zhu, W. Zheng, W. Wang and H.-B. Yang, *Chem. Soc. Rev.*, 2021, DOI: 10.1039/D0CS00654H.

8 (*a*) S. J. Loeb, *Chem. Soc. Rev.*, 2007, **36**, 226–235; (*b*) N. D. Suhan, L. Allen, M. T. Gharib, E. Viljoen, S. J. Vella and S. J. Loeb, *Chem. Commun.*, 2011, **47**, 5991–5993; (*c*) X. Yan, P. Wei, B. Xia, F. Huang and Q. Zhou, *Chem. Commun.*, 2012, **48**, 4968–4970; (*d*) S. Li, J. Huang, F. Zhou, T. R. Cook, X. Yan, Y. Ye, B. Zhu, B. Zheng and P. J. Stang, *J. Am. Chem. Soc.*, 2014, **136**, 5908–5911.

9 (*a*) X. Yan, D. Xu, X. Chi, J. Chen, S. Dong, X. Ding, Y. Yu and F. Huang, *Adv. Mater.*, 2012, **24**, 362; (*b*) G. Yu, X. Yan, C. Han and F. Huang, *Chem. Soc. Rev.*, 2013, **42**, 6697–6722; (*c*) S. Zhang, A. M. Bellinger, D. L. Glettig, R. Barman, Y. L. Lee, J. Zhu, C. Cleveland, V. A. Montgomery, L. Gu, L. D. Nash, D. J. Maitland, R. Langer and G. Traverso, *Nat. Mater.*, 2015, **14**, 1065–1071; (*d*) H. Nie, N. S. Schauser, J. L. Self, T. Tabassum, S. Oh, Z. Geng, S. D. Jones, M. S. Zayas, V. G. Reynolds, M. L. Chabinyc, C. J. Hawker, S. Han, C. M. Bates, R. A. Segalman and J. Read de Alaniz, *J. Am. Chem. Soc.*, 2021, **143**, 1562–1569.